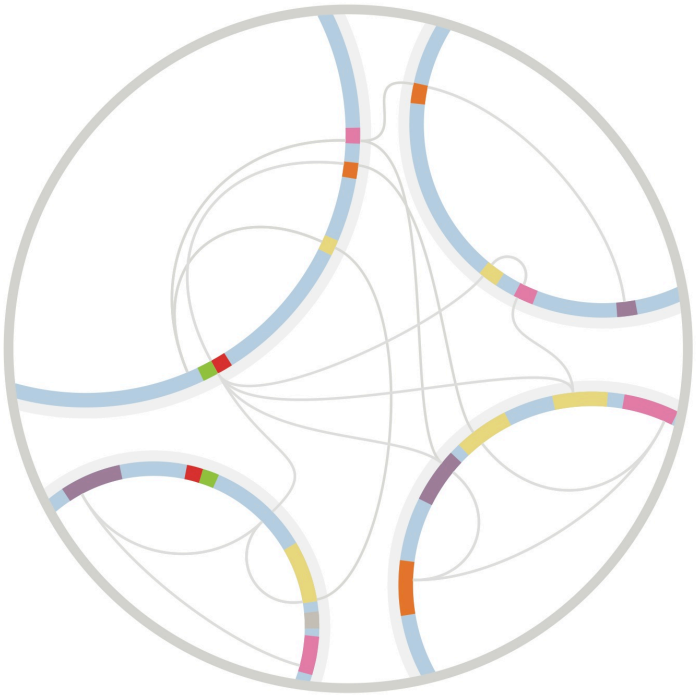

Convergence of dispersed regulatory mutations reveals candidate driver genes in prostate cancer

Richard Sallari | Manolis Kellis Lab | MIT & Broad

Regulatory plexus convergence model

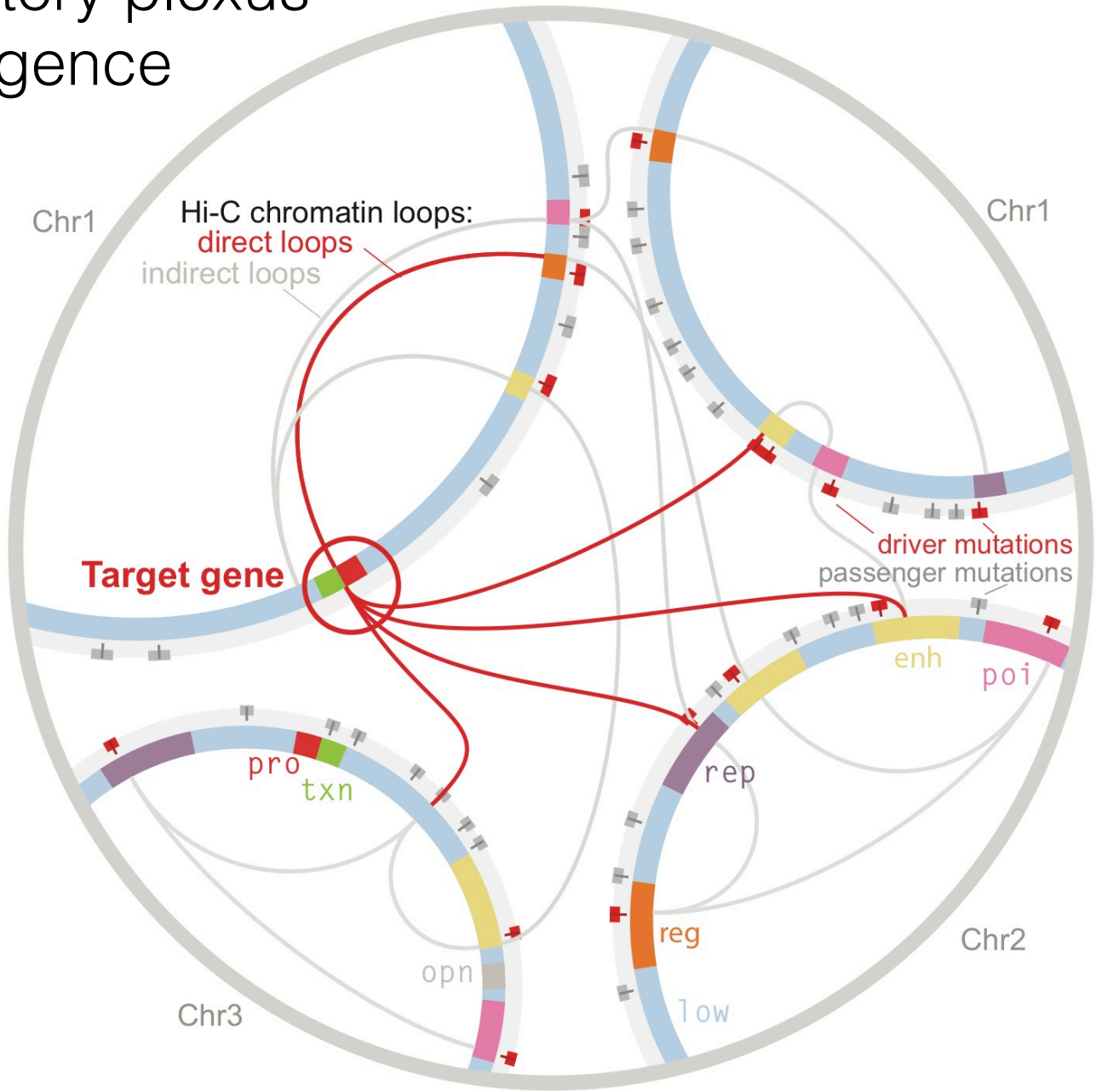

Regulatory plexus convergence model

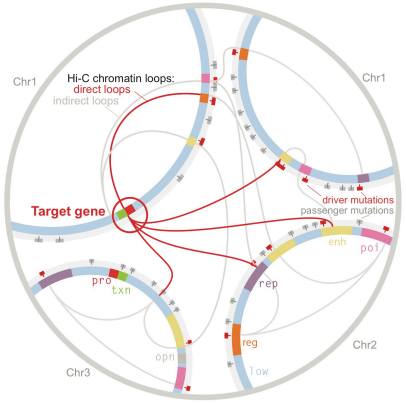

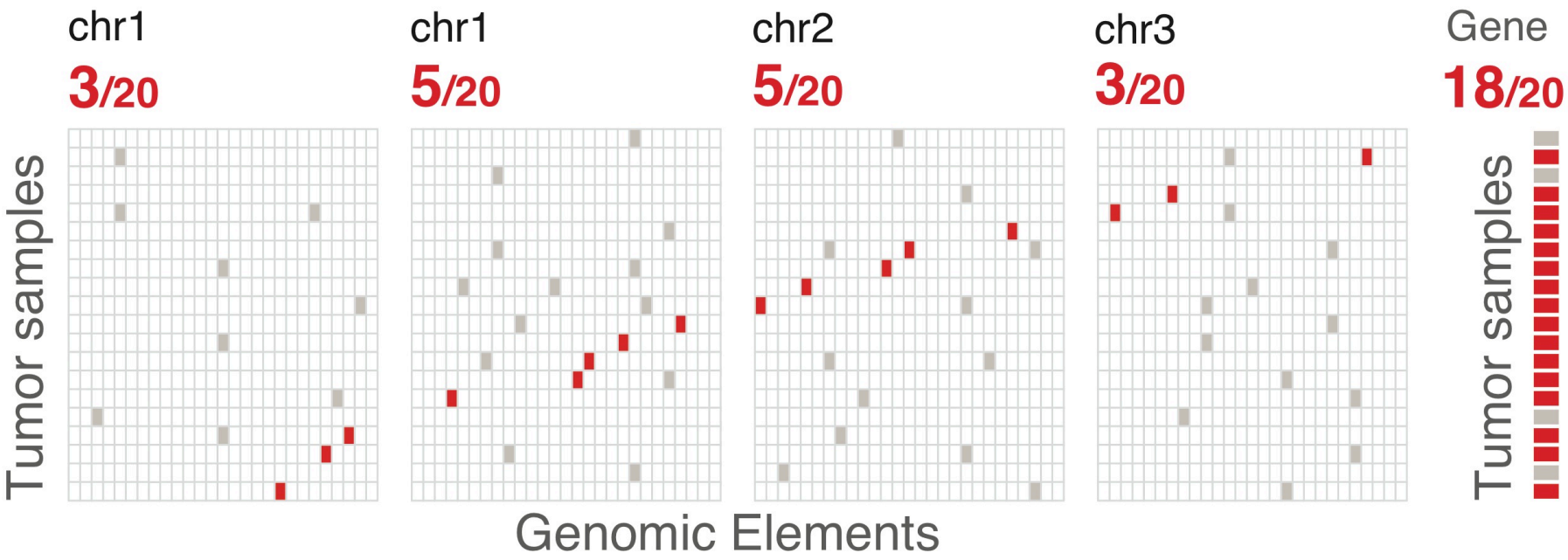

Some patterns of recurrence might be hard to detect.

Cell

Punctuated Evolution of Prostate Cancer Genomes

Sylvan C. Baca,[1,2,3] Davide Prandi,[6] Michael S. Lawrence,[2] Juan Miguel Mosquera,[6] Alessandro Romanel,[6] Yotam Drier,[2,7] Kyung Park,[8] Naoki Kitabayashi,[8] Theresa Y. MacDonald,[8] Mahmoud Ghandi,[2] Eliezer Van Allen,[2,3] Gregory V. Kryukov,[1,2,13] Andrea Sboner,[8,9] Jean-Philippe Theurillat,[2] T. David Soong,[9] Elizabeth Nickerson,[2] Daniel Auclair,[2] Ashutosh Tewari,[10,11] Himisha Beltran,[12] Robert C. Onofrio,[2] Gunther Boysen,[8] Candace Guiducci,[2] Christopher E. Barbieri,[8,11] Kristian Cibulskis,[2] Andrey Sivachenko,[2] Scott L. Carter,[2] Gordon Saksena,[2] Douglas Voet,[2] Alex H. Ramos,[1,2] Wendy Winckler,[2] Michelle Cipicchio,[2] Kristin Ardlie,[2] Philip W. Kantoff,[1,3] Michael F. Berger,[14] Stacey B. Gabriel,[2] Todd R. Golub,[2,4,5,15] Matthew Meyerson,[1,2,3,4] Eric S. Lander,[1,2,16,17] Olivier Elemento,[9] Gad Getz,[2] Francesca Demichelis,[6,9,18,*] Mark A. Rubin,[8,11,18] and Levi A. Garraway[1,2,3,4,18,*]
[1]Harvard Medical School, Boston, MA 02115, USA
[2]The Broad Institute of Harvard and MIT, Cambridge, MA 02142, USA
[3]Department of Medical Oncology
[4]Center for Cancer Genome Discovery
[5]Department of Pediatric Oncology
Dana-Farber Cancer Institute, Boston, MA 02215, USA
[6]Centre for Integrative Biology, University of Trento, Povo, Trento 38123, Italy
[7]Department of Physics of Complex Systems, Weizmann Institute of Science, Rehovot 76100, Israel
[8]Department of Pathology and Laboratory Medicine
[9]Institute for Computational Biomedicine, Department of Physiology and Biophysics
[10]Lefrak Center of Robotic Surgery and Center for Prostate Cancer Research & Clinical Care
[11]Brady Foundation Department of Urology
[12]Department of Medicine, Division of Hematology and Medical Oncology
Weill Cornell Medical College, New York, NY 10065, USA
[13]Division of Genetics, Brigham and Women's Hospital, Boston, MA 02115, USA
[14]Department of Pathology, Memorial Sloan-Kettering Cancer Center, New York, NY 10065, USA
[15]Howard Hughes Medical Institute, Chevy Chase, MD 20815, USA
[16]Department of Biology, MIT, Cambridge, MA 02139, USA
[17]Whitehead Institute for Biomedical Research, Cambridge, MA 02142, USA
[18]These authors contributed equally to this work
*Correspondence: demichelis@science.unitn.it (F.D.), levi_garraway@dfci.harvard.edu (L.A.G.)
http://dx.doi.org/10.1016/j.cell.2013.03.021

SUMMARY

The analysis of exonic DNA from prostate cancers has identified recurrently mutated genes, but the spectrum of genome-wide alterations has not been profiled extensively in this disease. We sequenced the genomes of 57 prostate tumors and matched normal tissues to characterize somatic alterations and to study how they accumulate during oncogenesis and progression. By modeling the genesis of genomic rearrangements, we identified abundant DNA translocations and deletions that arise in a highly interdependent manner. This phenomenon, which we term "chromoplexy," frequently accounts for the dysregulation of prostate cancer genes and appears to disrupt multiple cancer genes coordinately. Our modeling suggests that chromoplexy may induce considerable genomic derangement over relatively few events in prostate cancer and other neoplasms, supporting a model of punctuated cancer evolution. By characterizing the clonal hierarchy of genomic lesions in prostate tumors, we charted a path of oncogenic events along which chromoplexy may drive prostate carcinogenesis.

INTRODUCTION

Though often curable at early stages, clinically advanced prostate cancer causes over 250,000 deaths worldwide annually (Jemal et al., 2011). Identifying prostate cancers that require aggressive treatment and gaining durable control of advanced disease comprise two pressing public health needs. A deeper understanding of the molecular genetic changes that occur during the development of invasive and metastatic tumors may provide useful insights into these problems.

Genetic studies of prostate cancer have revealed numerous recurrent DNA alterations that dysregulate genes involved in prostatic development, chromatin modification, cell-cycle regulation, and androgen signaling, among other processes (Baca and Garraway, 2012). Chromosomal deletions accumulate early in prostate carcinogenesis and commonly inactivate tumor suppressor genes (TSGs) such as *PTEN*, *TP53*, and *CDKN1B* (Shen and Abate-Shen, 2010). In addition, recent exome sequencing of

Baca … Garraway *Cell* 2013
55 Prostate cancer WGS

PNAS

Oncogene-mediated alterations in chromatin conformation

David S. Rickman[a,1], T. David Soong[b,1], Benjamin Moss[a], Juan Miguel Mosquera[a], Jan Dlabal[b], Stéphane Terry[a], Theresa Y. MacDonald[a], Joseph Tripodi[c], Karen Bunting[d], Vesna Najfeld[c], Francesca Demichelis[b,e], Ari M. Melnick[d,f], Olivier Elemento[b,2], and Mark A. Rubin[a,f,2,3]

Departments of [a]Pathology and Laboratory Medicine and [c]Medicine, [b]Department of Physiology and Biophysics, HRH Prince Alwaleed Bin Talal Bin Abdulaziz Alsaud Institute for Computational Biomedicine, and [d]Weill Cornell Cancer Center, Weill Cornell Medical College, New York, NY 10065; [f]Tumor Cytogenetics Laboratory, Department of Pathology, Tisch Cancer Center, Mount Sinai School of Medicine, New York, NY 10029; and [e]Centre for Integrative Biology, University of Trento, 38122 Trento, Italy

Edited* by Eric S. Lander, The Broad Institute of MIT and Harvard, Cambridge, MA, and approved April 24, 2012 (received for review August 3, 2011)

Emerging evidence suggests that chromatin adopts a nonrandom 3D topology and that the organization of genes into structural hubs and domains affects their transcriptional status. How chromatin conformation changes in diseases such as cancer is poorly understood. Moreover, how oncogenic transcription factors, which bind to thousands of sites across the genome, influence gene regulation by globally altering the topology of chromatin requires further investigation. To address these questions, we performed unbiased high-resolution mapping of intra- and interchromosome interactions upon overexpression of ERG, an oncogenic transcription factor frequently overexpressed in prostate cancer as a result of a gene fusion. By integrating data from genome-wide chromosome conformation capture (Hi-C), ERG binding, and gene expression, we demonstrate that oncogenic transcription factor overexpression is associated with global, reproducible, and functionally coherent changes in chromatin organization. The results presented here have broader implications, as genomic alterations in other cancer types frequently give rise to aberrant transcription factor expression, e.g., EWS-FLI1, c-Myc, n-Myc, and PML-RARα.

Mounting evidence suggests that many genes dynamically colocalize to shared nuclear compartments that favor gene activation or silencing (1–3). As demonstrated by chromosome conformation capture (3C) (4), ligand-bound androgen receptors (AR) and estrogen receptors mediate looped chromatin structures resulting in coordinated transcription of target genes (5, 6). In embryonic carcinoma cells, the PolyComb complex subunit EZH2 represses some of its target genes via the formation of similar looped chromatin structures (7). *Trans*-interactions that regulate gene expression have also been reported (8–10). These data suggest that oncogenic transcriptional regulators are capable of inducing changes in chromatin structures. These studies have mainly focused on local chromatin structures, and it is still unclear whether more global changes occur in the process of oncogene-mediated transformation. A broader implication of these observations is that global chromatin organization changes could impact functional and phenotypic aspects of cancer.

To globally investigate oncogene-mediated chromatin structure changes we focused on ERG, the *ETS*-family transcription factor most frequently rearranged and overexpressed in prostate cancer through the *TMPRSS2-ERG* and other gene fusions involving androgen-responsive promoters (11–13). ERG interacts with several cofactors (14) and other transcription factors including AR to regulate the expression of thousands of genes that favor dedifferentiation, cell invasion, and neoplastic transformation of prostate epithelium when overexpressed (15–20). We therefore hypothesized that changes in global gene expression induced by ERG overexpression could be associated with global changes in the 3D structure of chromosomes.

Results

ERG Overexpression Is Associated with Chromatin Topology. To test our hypothesis, we used stable isogenic, normal benign prostate epithelial cell lines (RWPE1) (21) that differ with respect to ERG overexpression (17) (Fig. S1*A*). To test whether ERG overexpression is associated with global changes in chromatin structure, we performed unbiased chromatin interaction mapping using the Hi-C technique (22) from both RWPE1-ERG and RWPE1-GFP cells, with biological replicates (Fig. 1*A* and Fig. S1*A*). Successful fill-in and ligation were determined as previously reported (22) by testing for a known interaction between two distant genomic loci located on chromosome 6 (23) (Fig. S1*B*). The Hi-C libraries were paired-end sequenced using an Illumina GAIIx platform. Following alignment to the human genome (hg18) and filtering to remove unligated and self-ligated DNA, we identified intrachromosomal (or *cis*-) and interchromosomal (or *trans*-) interactions in both RWPE1 cell lines. Correlation matrices obtained from independent biological replicates were highly similar in both cell lines (Pearson's correlation coefficient $r = 0.99$), indicating that the interaction patterns are highly reproducible. Biological replicate interactions were therefore combined for further analyses. In total, we identified 18.4 million intrachromosomal (or *cis*-) and 18.3 million interchromosomal (or *trans*-) interactions in RWPE1-ERG cells (Dataset S1). We also identified 16.9 million *cis*- and 18.6 million *trans*-interactions in RWPE1-GFP cells.

To visualize global patterns of *cis*-interactions, we binned the genome (chromosomes 1–22, X) into 1-Mb intervals and calculated the ratio between observed and expected number of interactions connecting each interval pair. We then generated correlation heat maps depicting the extent to which pairs of genomic intervals interact with the same intervals, on the basis of the assumption that if two loci are close in nuclear space, their patterns of interaction with other loci should be highly correlated. Confirming prior observations (22), the heat maps showed

Author contributions: D.S.R., T.D.S., O.E., and M.A.R. designed research; D.S.R., T.D.S., B.M., J.D., S.T., T.Y.M., J.T., V.N., and O.E. performed research; T.D.S., K.B., F.D., A.M.M., and O.E. contributed new reagents/analytic tools; D.S.R., T.D.S., B.M., J.M.M., J.D., S.T., J.T., V.N., O.E., and M.A.R. analyzed data; and D.S.R., T.D.S., J.D., S.T., O.E., and M.A.R. wrote the paper.

The authors declare no conflict of interest.

*This Direct Submission article had a prearranged editor.

Freely available online through the PNAS open access option.

Data deposition: Hi-C and ChIPseq data reported in this paper have been deposited in the Gene Expression Omnibus (GEO) database, www.ncbi.nlm.nih.gov/geo (accession no. GSE37752).

[1]D.S.R. and T.D.S. contributed equally to this work.

[2]O.E. and M.A.R. contributed equally to this work.

[3]To whom correspondence should be addressed. E-mail: rubinma@med.cornell.edu.

This article contains supporting information online at www.pnas.org/lookup/suppl/doi:10.1073/pnas.1112570109/-/DCSupplemental.

Rickman … Rubin *PNAS* 2012
Prostate Hi-C (RWPE1)

Generate chromatin states in prostate (RWPE1) and mutation rates in prostate cancer

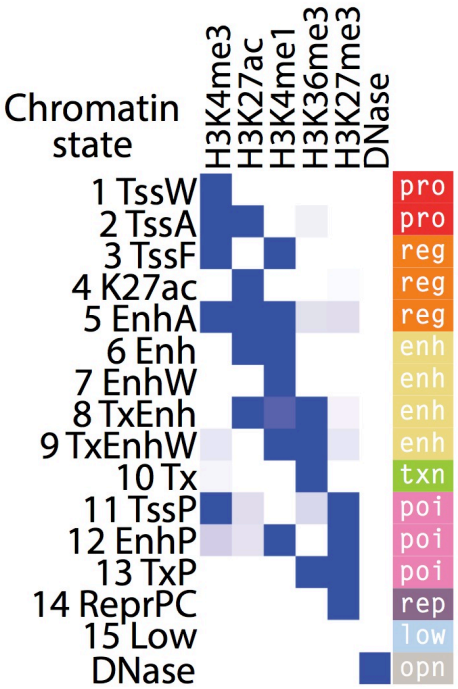

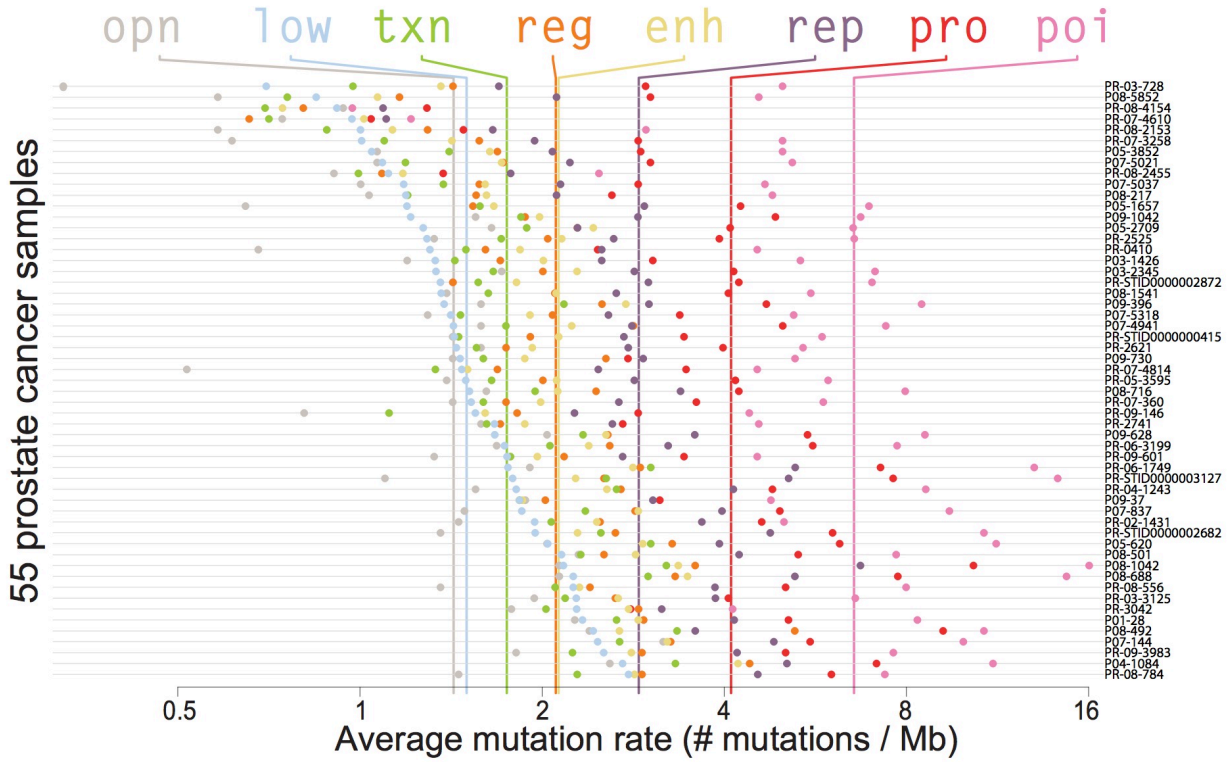

Ken Kron and
Mathieu Lupien
(University of Toronto)

Chromatin states have different mutation rates.

Assemble gene plexi in normal prostate (RWPE1)

Elements

opn	pro	reg	enh	txn	poi	rep	low	
21	9	13	41	7	4	8	41	proximal
280	119	170	557	116	76	186	717	distal_cis
350	142	211	723	162	109	280	1,011	distal_trans

Bases

opn	pro	reg	enh	txn	poi	rep	low	
4,000	4,300	6,600	29,300	11,300	2,700	8,200	136,100	proximal
52,400	55,300	87,700	385,750	160,400	47,000	199,100	2,622,350	distal_cis
65,900	67,100	108,000	493,200	210,750	68,100	281,400	3,983,150	distal_trans

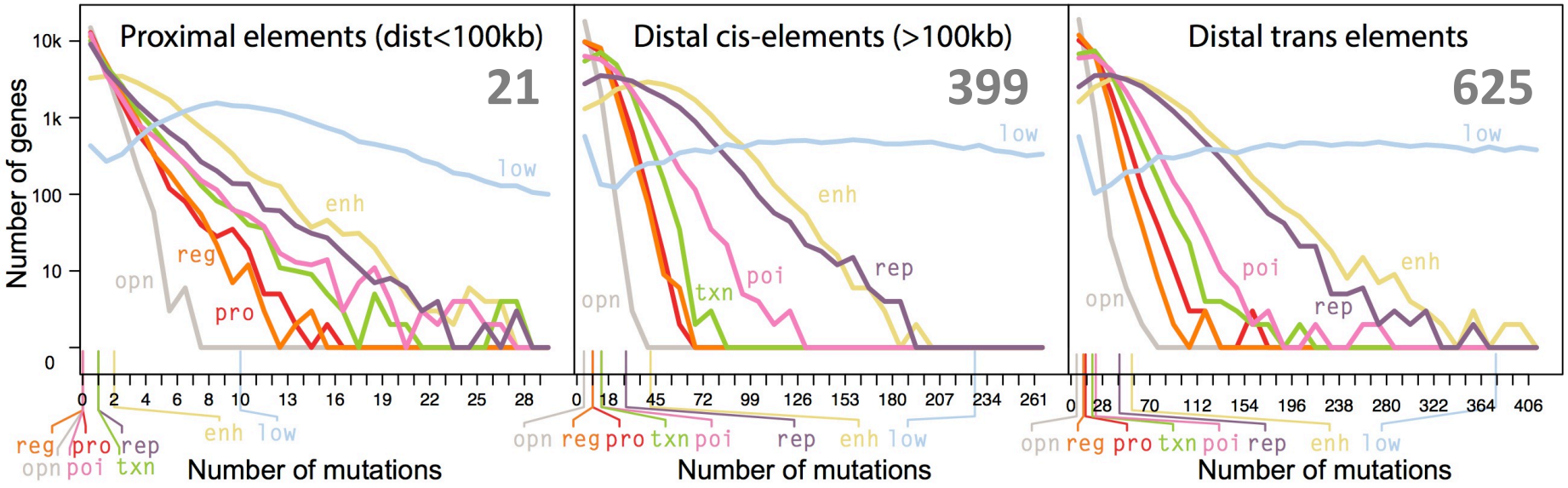

Gene plexi are large and heterogeneous

Regional heterogeneity

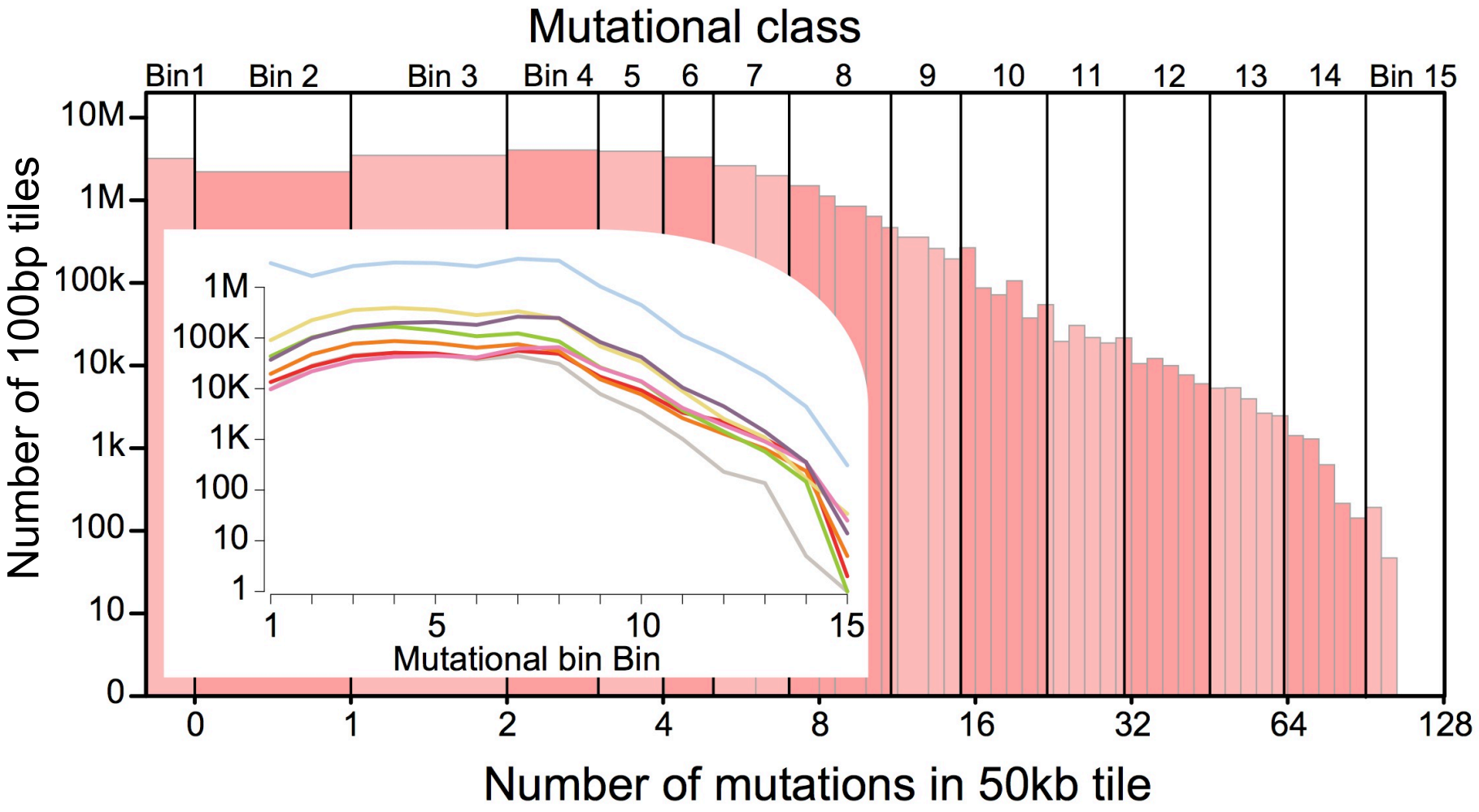

Regional mutation rates at the 50kb scale follow a power-law distribution

Plexus tile decomposition & mutation tally

Observed number of tiles in each state and mutation rate bin for ITM2A

	Bin1	Bin2	Bin3	Bin4	Bin5	Bin6	Bin7	Bin8	Bin9	Bin10	Bin11	Bin12	Bin13	Bin14	Bin15
opn	12	32	37	28	52	33	13	23	8	0	2	0	0	0	0
pro	6	61	78	68	73	55	78	75	17	1	0	0	0	0	0
reg	16	38	115	41	54	90	34	34	9	3	0	0	0	0	0
enh	95	227	274	263	239	186	162	238	85	23	13	0	0	0	0
txn	82	160	339	236	177	105	36	65	32	1	0	0	0	0	0
poi	6	66	59	19	36	37	76	69	65	7	8	0	0	0	0
rep	12	52	64	127	173	219	299	306	90	52	1	0	0	0	0
low	1281	3710	5255	5693	5635	4460	6060	5891	1166	338	233	0	0	0	0

Observed number of mutations in each state for each patient for ITM2A

	P01-28	P03-1426	P03-2345	P04-1084	P05-1657	P05-2709	P05-3852	P05-620	P07-144	P07-4941	P07-5021	P07-5037	P07-5318	P07-837	P08-1042	P08-1541	P08-217	P08-492	P08-501	P08-5852	P08-688	P08-716	P09-1042	P09-37	P09-396	P09-628	P09-730	PR-02-1431	PR-03-3125	PR-03-728	PR-04-1243	PR-0410	PR-05-3595	PR-06-1749	PR-06-3199	PR-07-3258	PR-07-360	PR-07-4610	PR-07-4814	PR-08-2153	PR-08-2455	PR-08-4154	PR-08-556	PR-08-784	PR-09-146	PR-09-3983	PR-09-601	PR-2525	PR-2621	PR-2741	PR-3042	PR-STID0000000415	PR-STID0000002682	PR-STID0000000287	PR-STID0000003127
opn	0	0	0	0	0	0	0	0	0	0	0	0	1	0	0	0	0	0	0	0	0	0	0	0	0	0	0	0	0	0	0	0	0	0	0	0	0	0	0	0	0	0	0	0	0	0	0	0	0	0	0	0	0	0	0	0
pro	0	0	0	0	0	0	0	0	0	1	0	0	0	0	1	0	0	0	0	0	0	1	0	2	0	0	0	1	0	0	0	0	0	0	1	0	0	0	0	0	0	0	0	0	0	0	0	0	2	0	0	0	0	0	1	0
reg	0	0	0	0	0	0	0	0	0	0	0	0	0	0	0	0	0	0	0	0	0	0	0	0	0	0	0	0	0	0	0	0	0	0	0	0	0	0	1	0	0	0	0	0	0	0	0	0	0	0	0	0	0	0	0	0
enh	3	1	1	0	1	3	0	5	0	4	1	0	1	0	1	3	1	2	2	0	1	0	1	0	0	3	2	0	0	0	1	0	2	4	1	2	1	0	0	0	1	0	0	0	0	0	2	2	1	0	0	2	0	1	2
txn	2	0	0	0	0	1	0	1	0	0	0	0	0	0	0	0	0	0	0	0	1	1	0	0	0	0	0	1	0	0	0	0	0	0	0	1	0	0	0	0	1	0	0	1	1	0	1	0	0	0	0	0	0	1	1	0
poi	1	0	0	2	1	0	0	0	1	0	0	1	1	0	0	0	0	0	1	0	1	3	0	0	0	1	0	0	0	0	0	0	0	0	0	0	0	0	0	0	0	0	0	0	1	1	0	0	1	1	0	0	0	0	0	0
rep	0	0	0	3	1	1	0	2	4	1	2	0	0	3	2	0	0	1	1	0	1	1	0	0	0	0	2	0	1	2	0	0	0	0	2	0	0	0	0	0	1	1	0	1	0	4	0	1	0	1	0	1	0	1	0	1	0
low	13	4	1	15	3	3	3	12	11	4	3	4	5	12	10	1	10	12	7	1	13	10	4	8	2	8	2	7	5	0	6	4	4	4	5	1	3	4	10	5	3	1	6	10	6	7	5	1	7	7	4	8	7	6	2
exn	0	0	0	0	0	0	0	0	0	0	0	0	0	0	0	0	0	0	0	0	0	0	0	0	0	0	0	0	0	0	0	0	0	0	0	0	0	0	0	0	0	0	0	0	0	0	0	0	0	0	0	1	0	0	0	0

Plexus mutational heterogeneity serves as input to permutation test

Plexus recurrence test

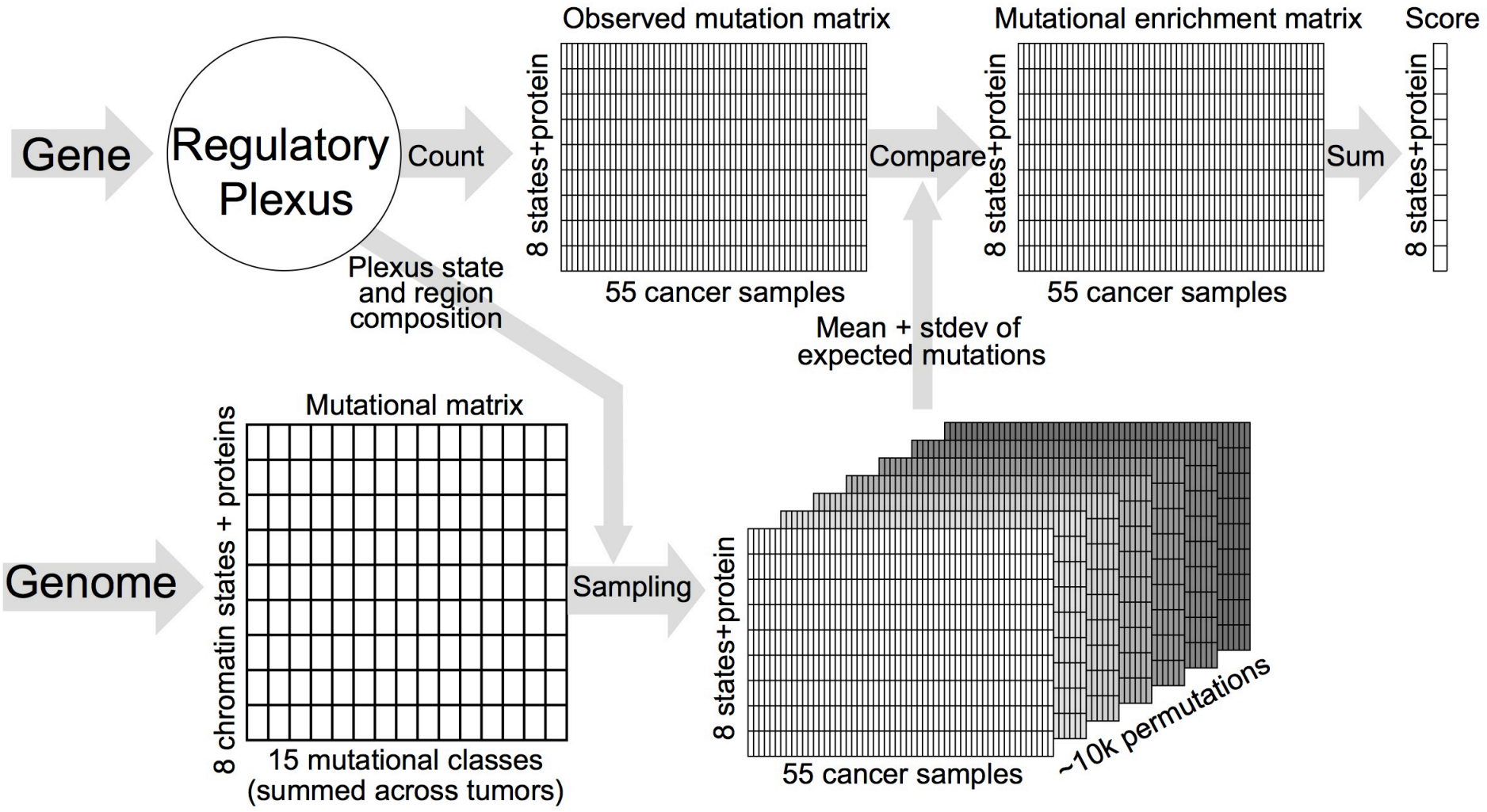

Tiles are sampled from the genome to match plexus decomposition matrix

Plexus recurrence test

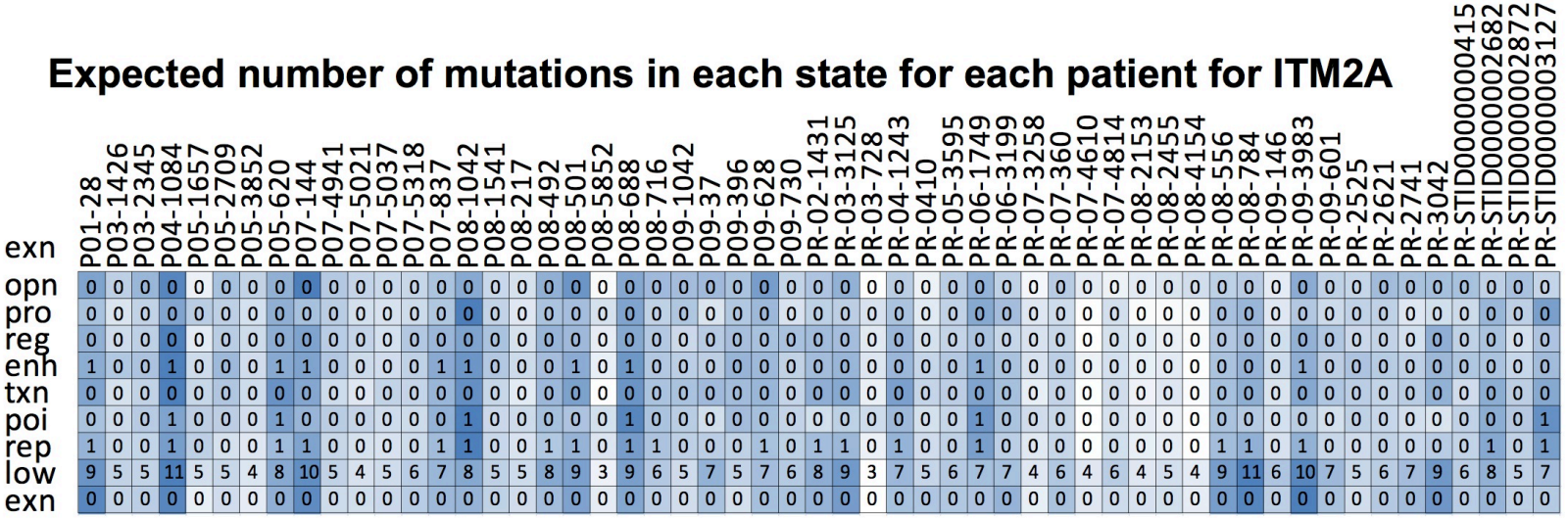

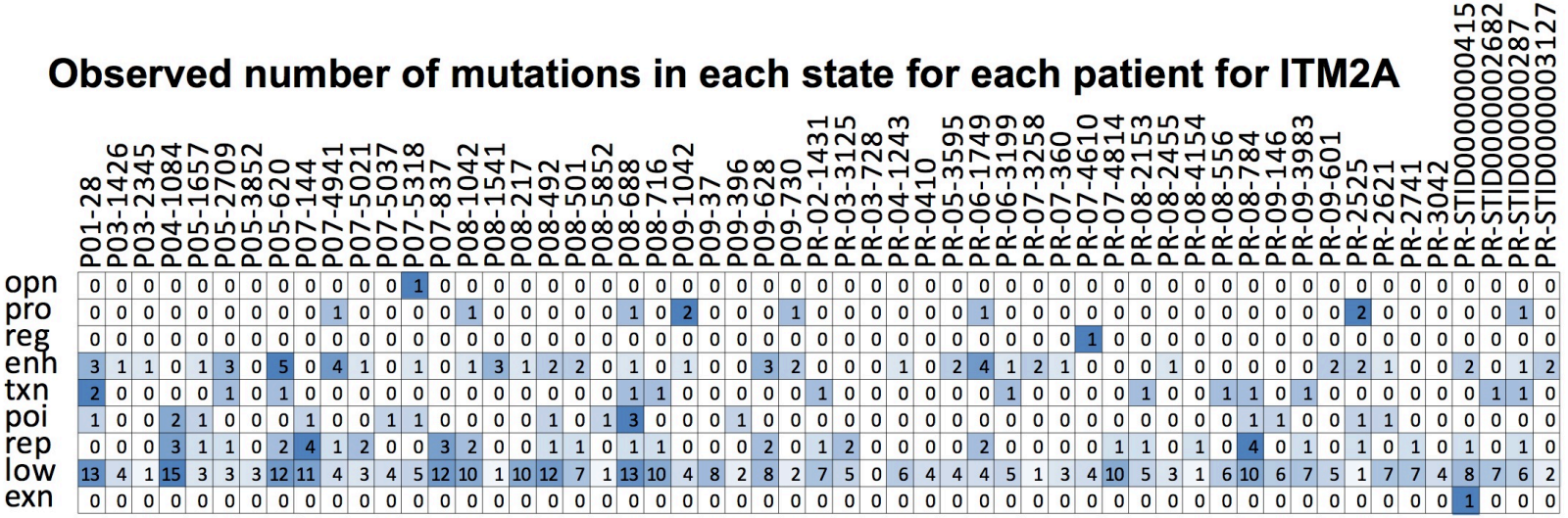

Through permutation we estimate the expected number of mutations per patient and chromatin state combination

Plexus recurrence test

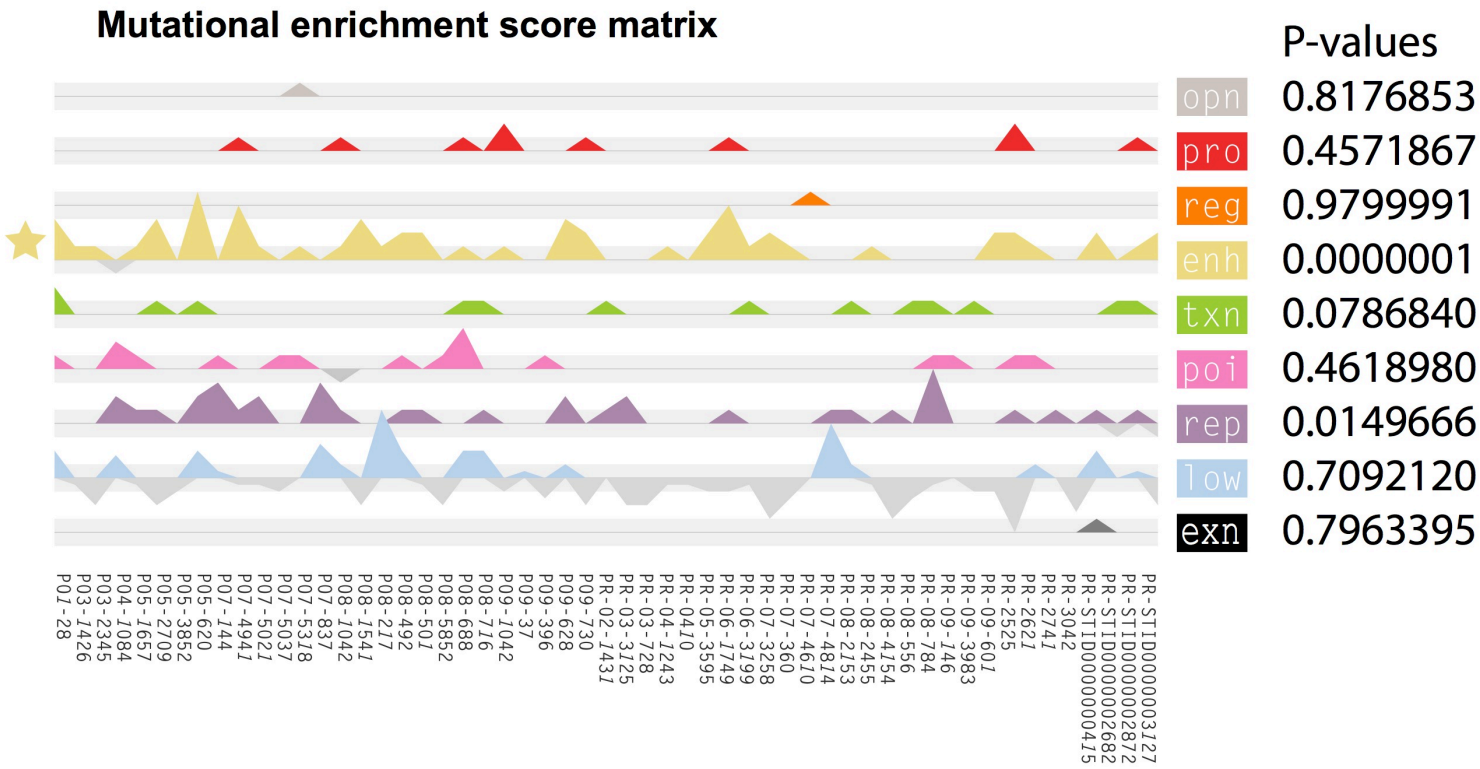

Mutation tallies for each chromatin state and annotation are normalized and tested independently

Plexus visualization

Nicholas Sinnott-Armstrong

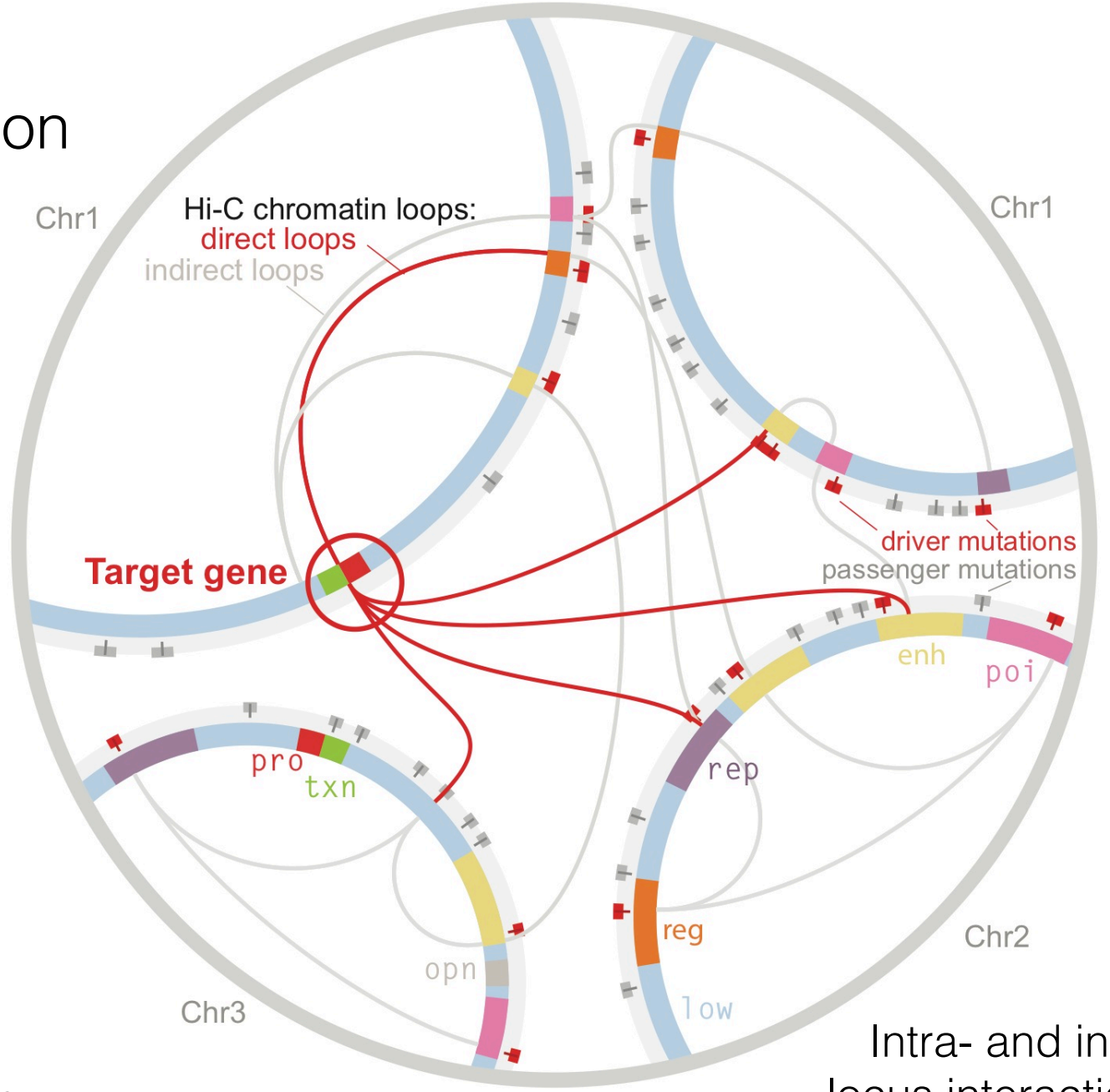

Intra- and inter-locus interactions

ITM2A plexus

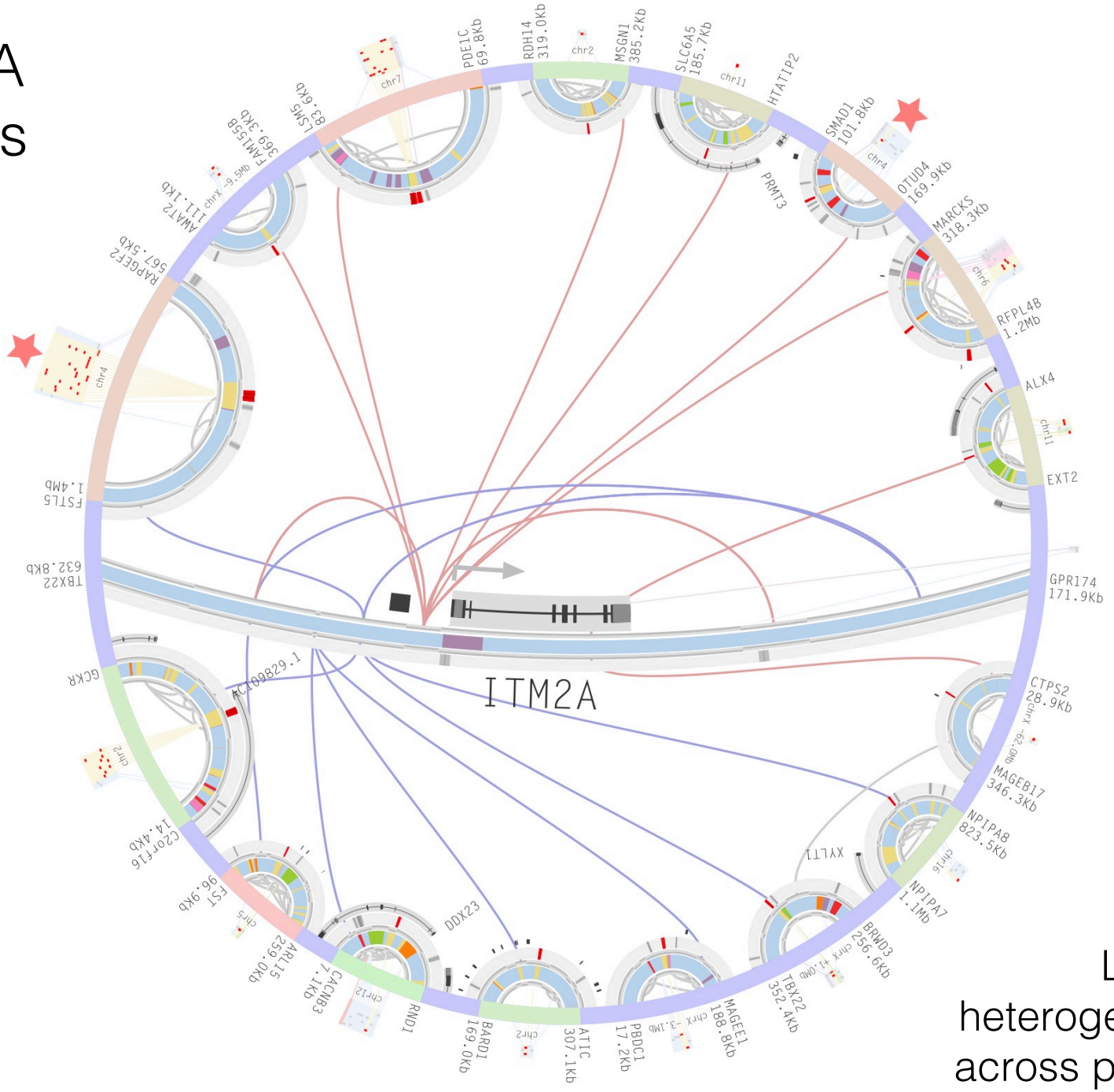

Locus heterogeneity across plexus

Plexus visualization: scallops

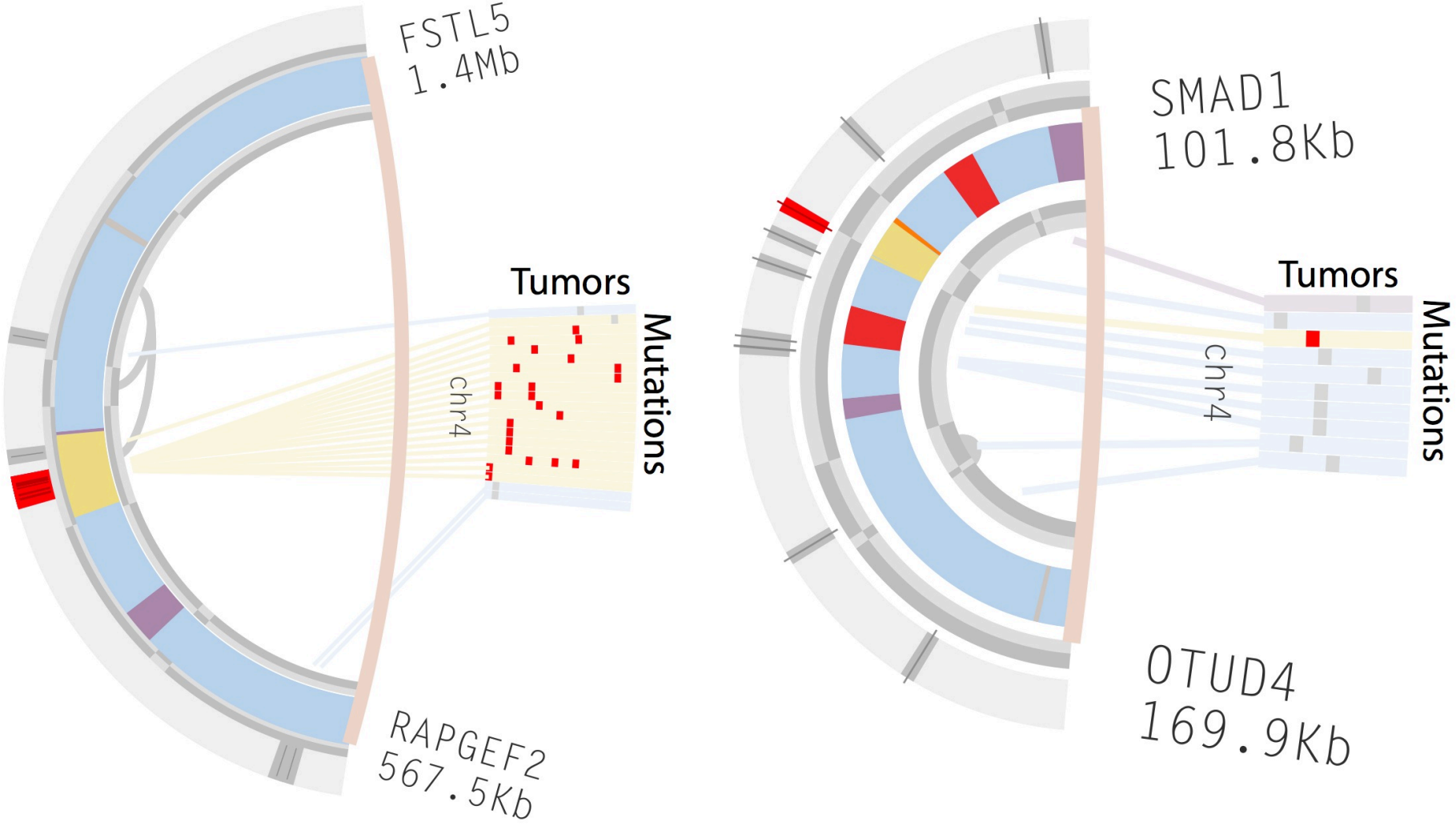

Mutational heterogeneity across patients

Cancer plexi in prostate cancer

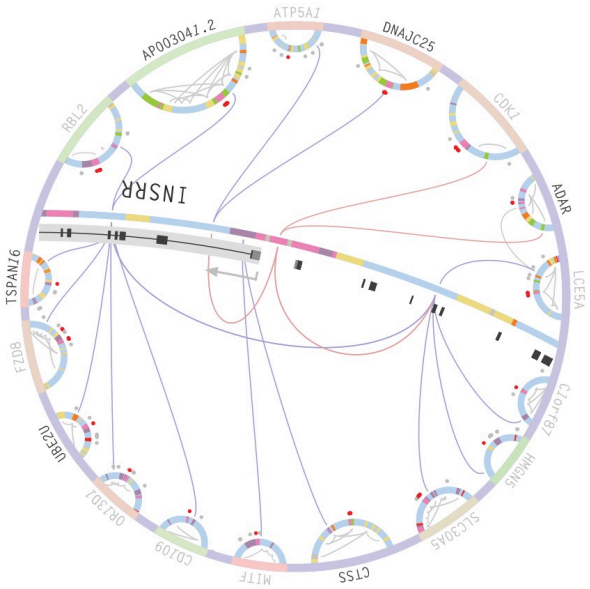

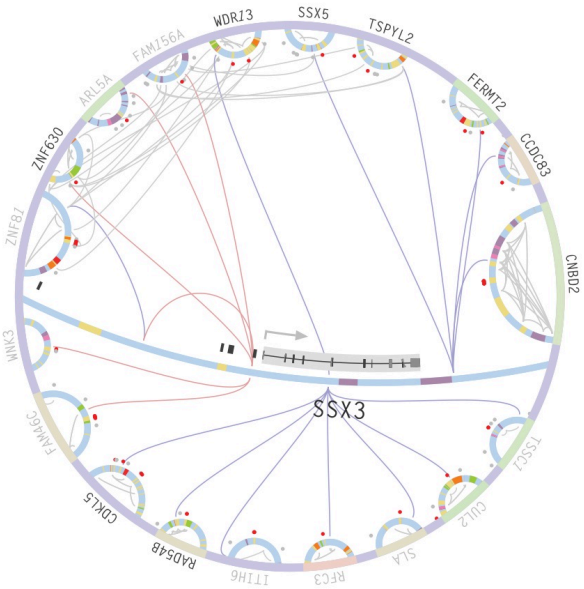

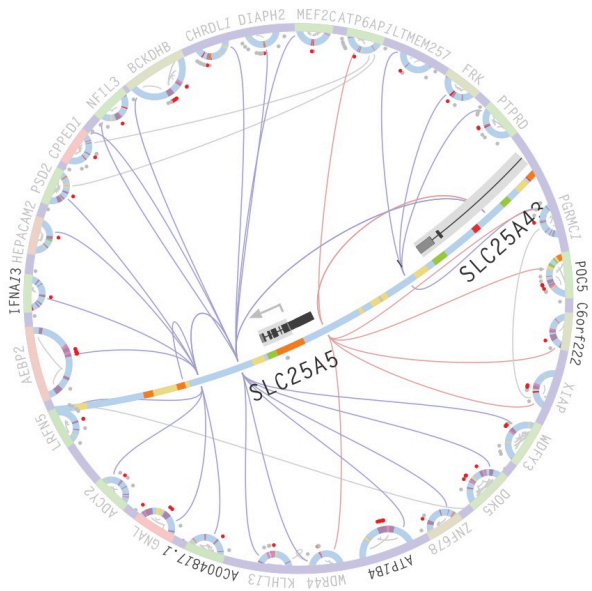

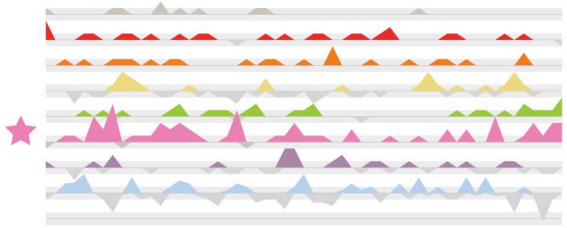

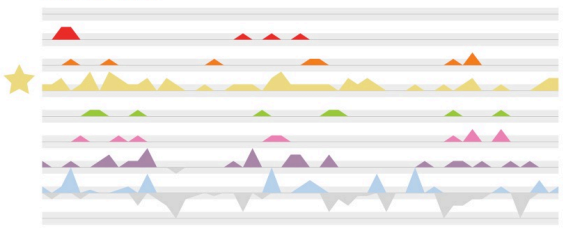

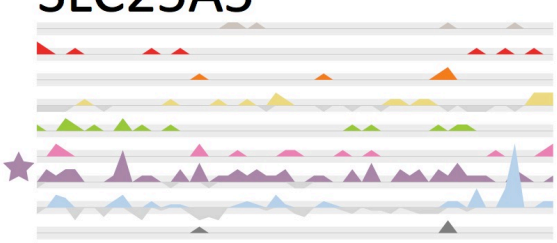

Mutational enrichment is chromatin-state-specific

Cancer plexi in prostate cancer

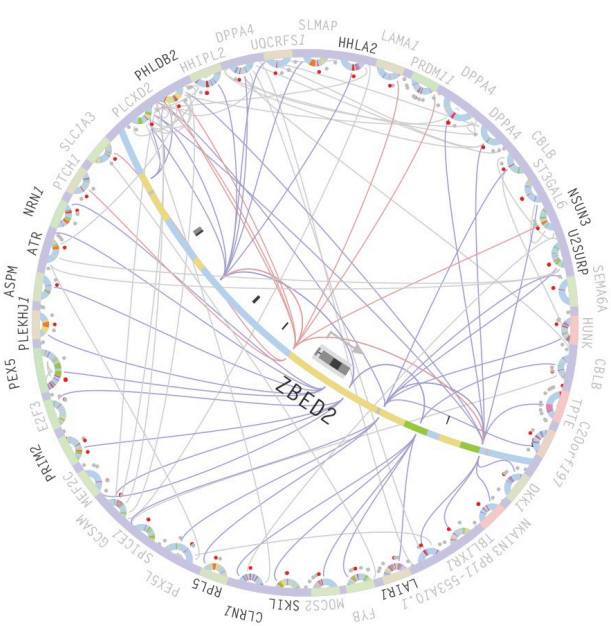

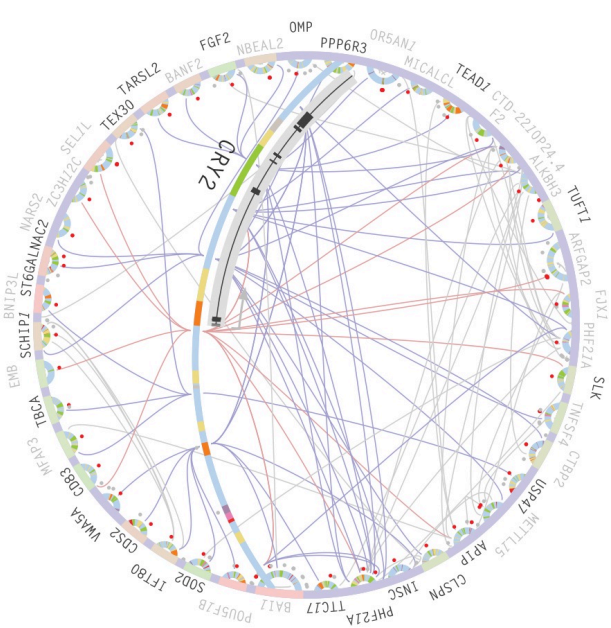

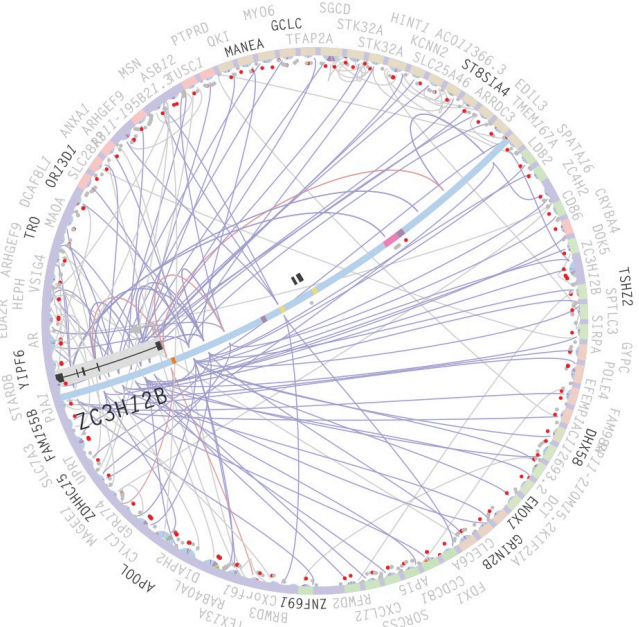

ZBED2

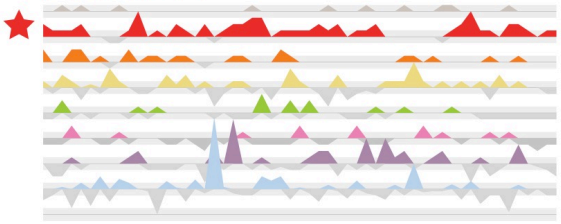

CRY2

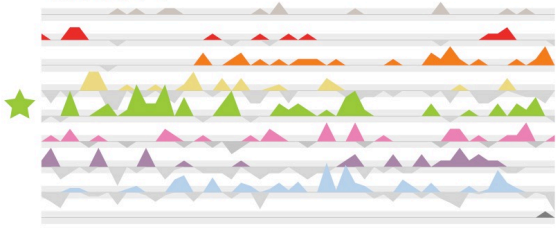

ZC3H12B

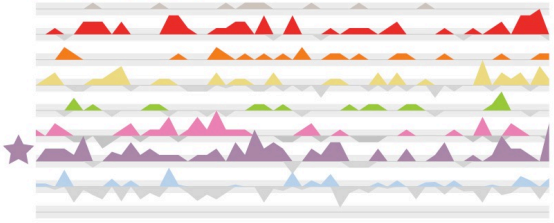

Plexi vary in structural complexity

Cancer plexi in prostate cancer

	Enriched chromatin state							All regulatory chromatin states					Panel	ConvGrp
Gene	State	P-val.	Nmut	Nelmt	Nchr	CnvElmt	CnvPlex	Nmut	Nelmt	Nchr	CnvElmt	CnvPlex	Gene function	
ITM2A	enh	1E-07	58	16	9	24%	56%	129	36	12	25%	87%	immun-evas	(2)
INSRR	poi	2E-07	76	17	11	22%	62%	267	89	22	38%	100% (b)	ins-androgen	(1)
ZCCHC16	txn	3E-07	63	25	17	29%	60%	275	115	23	33%	98%	unknown	N/A
ZBED2	pro	9E-07	72	35	13	18%	71%	421	143	22	62%	100% (e)	immun-evas	(2)
SPANXN3	pro	1E-06	24	7	4	9%	35%	124	55	17	22%	85%	spermatogen	(1)
PLCB4	txn	2E-06	79	24	14	18%	67%	362	113	23	62%	98%	ins-androgen	(1)
COQ3	pro	2E-06	58	28	11	16%	64%	326	115	22	49%	100%	mitochondr	(3)
EDNRA	txn	2E-06	102	37	14	18%	75%	392	143	21	76%	100%	blood flow	N/A
CRY2	txn	3E-06	83	34	13	20%	65%	289	118	20	60%	100% (f)	ins-androgen	(1)
ZC3H12B	rep	3E-06	150	62	16	36%	89%	415	141	23	71%	100% (g)	immun-evas	(2)
C14orf180	txn	4E-06	49	16	11	11%	51%	142	52	20	55%	93%	secreted	N/A
IDO2	rep	4E-06	98	45	17	22%	87%	189	72	19	47%	98%	immun-evas	(2)
RRAD	poi	4E-06	47	13	8	20%	51%	180	57	19	55%	95%	ins-androgen	(1)
SLC25A5	rep	4E-06	68	27	12	18%	67%	143	50	17	29%	91% (d)	mitochondr	(3)
SSX3	enh	4E-06	53	14	9	25%	65%	104	31	17	25%	78% (c)	spermatogen	(1)

Genes converge at the pathway level

Acknowledgments

Manolis Kellis (MIT CSAIL Broad)
Nicholas Sinnott-Armstrong (MIT CSAIL Broad)
Mathieu Lupien (University of Toronto)
Jason Moore (Dartmouth College)
Zhizhuo Zhang (MIT CSAIL Broad)
Ken Kron (University of Toronto)
Levi Garraway (DFCI HMS Broad)
Sylvan Baca (DFCI HMS Broad)

Plexus mutations in dysregulated genes

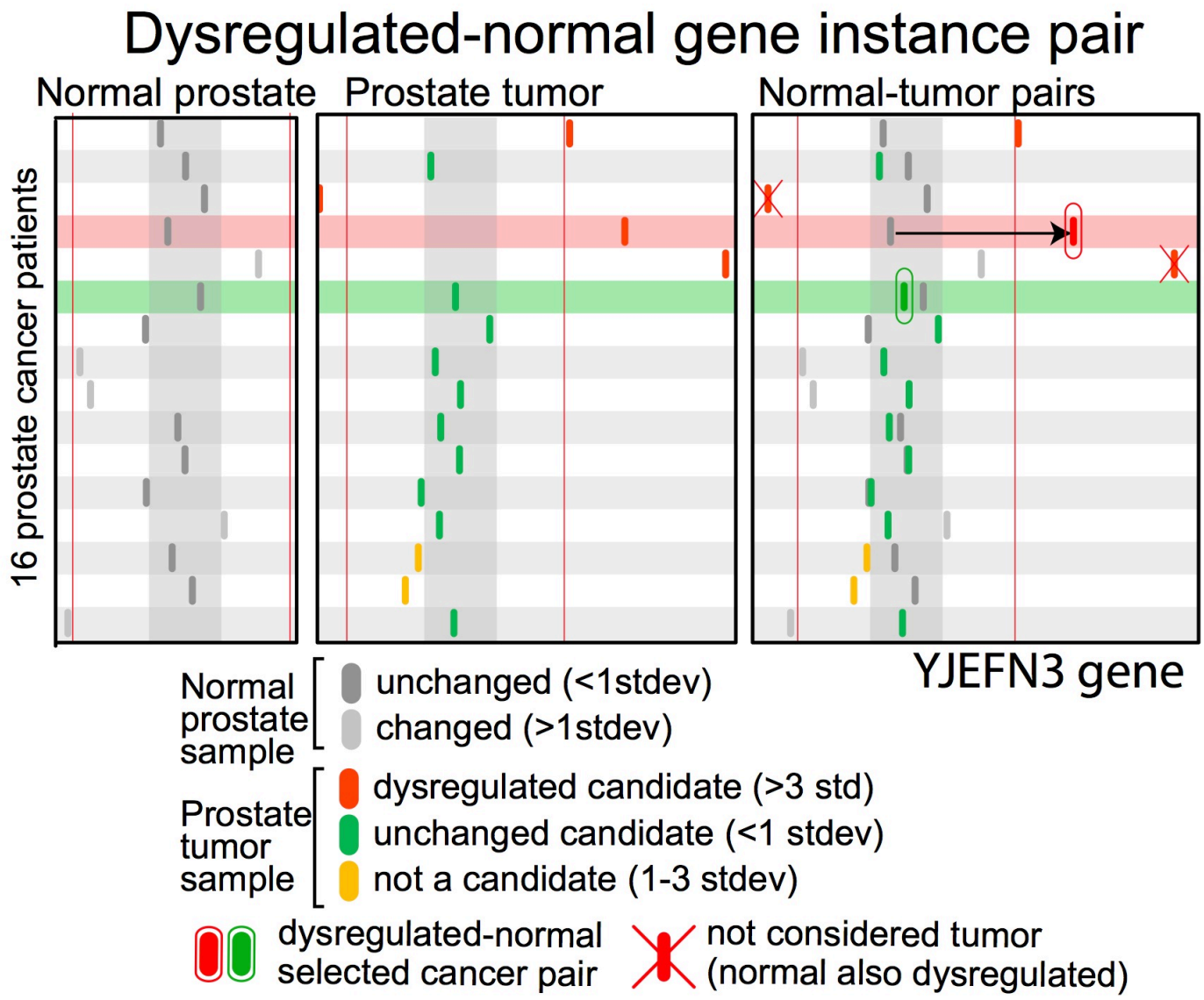

Plexus mutations in dysregulated genes

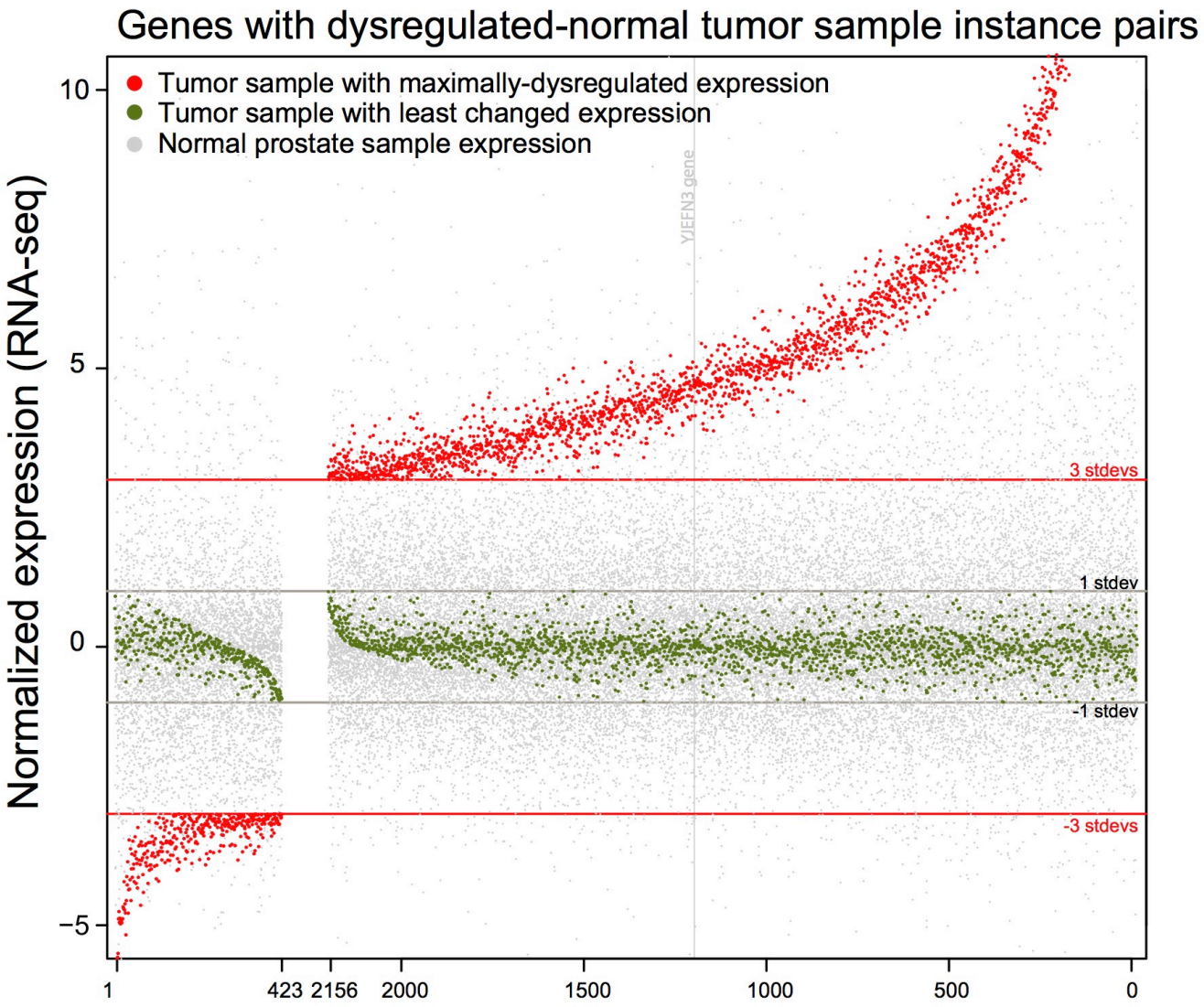

Plexus mutations in dysregulated genes

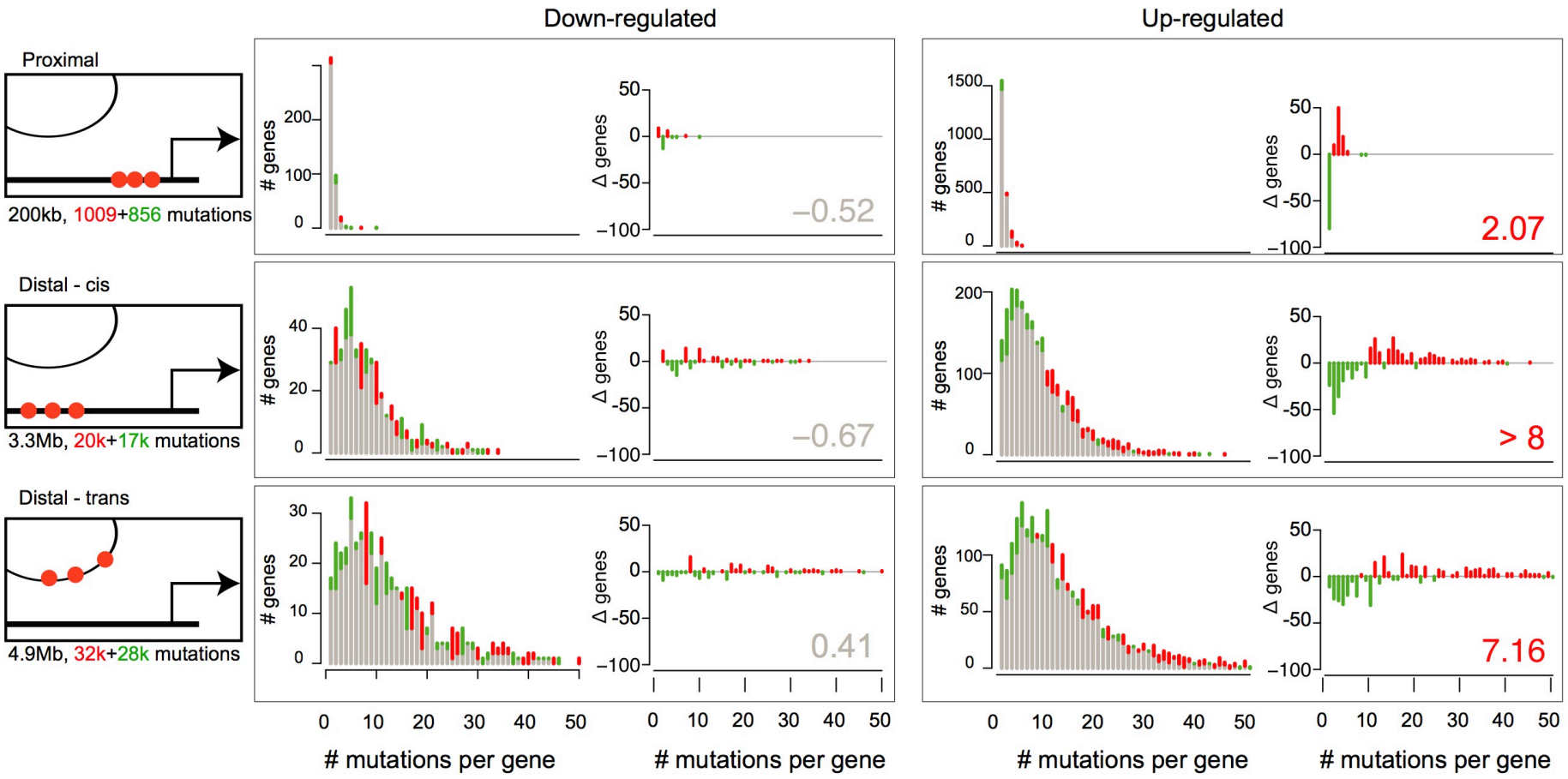

Dysregulated genes are enriched for plexus mutations at all distances.

Plexus mutations in dysregulated genes

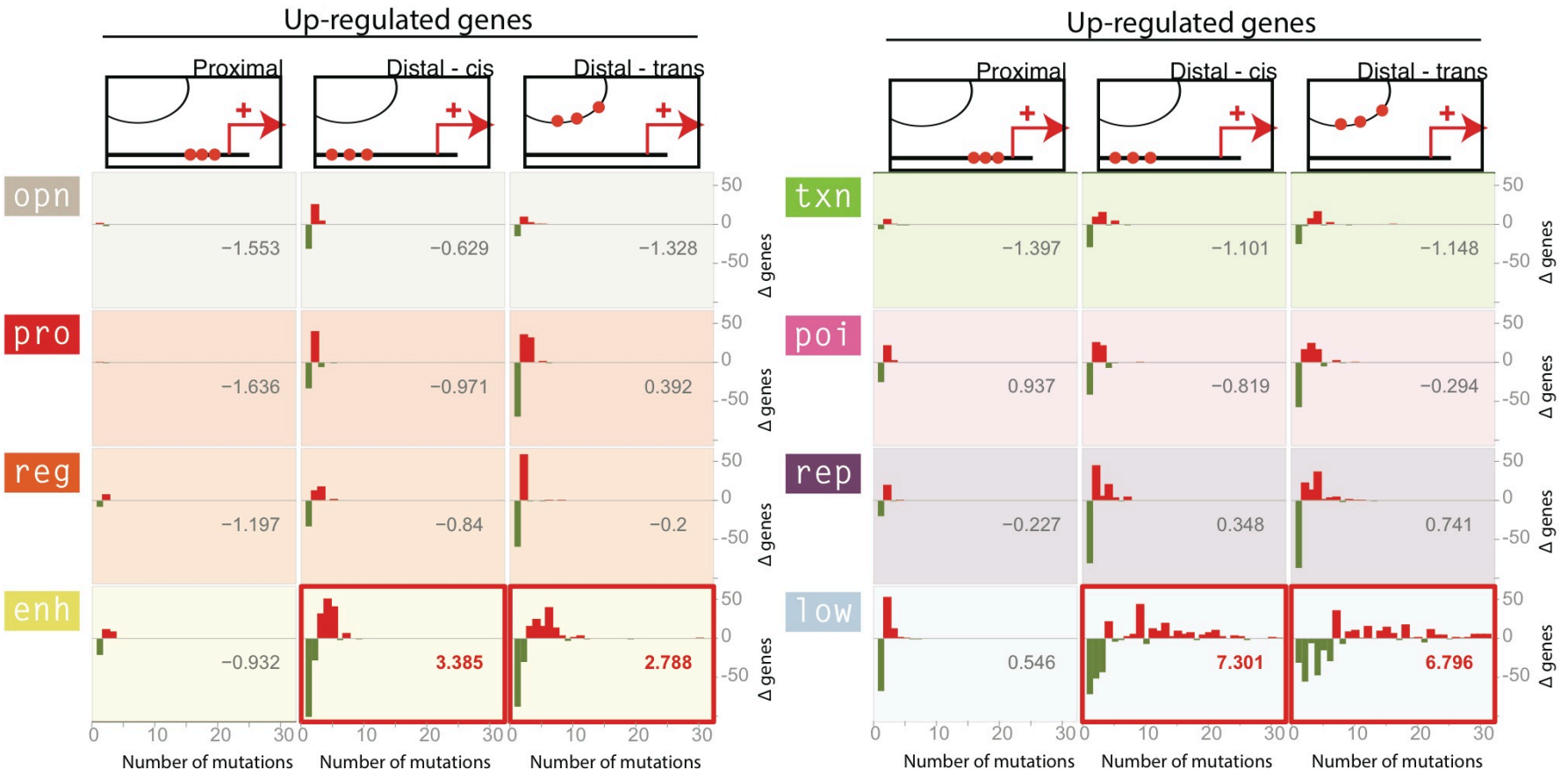

Mutations are enriched in enhancers and low regions.

Out-of-context de-repression

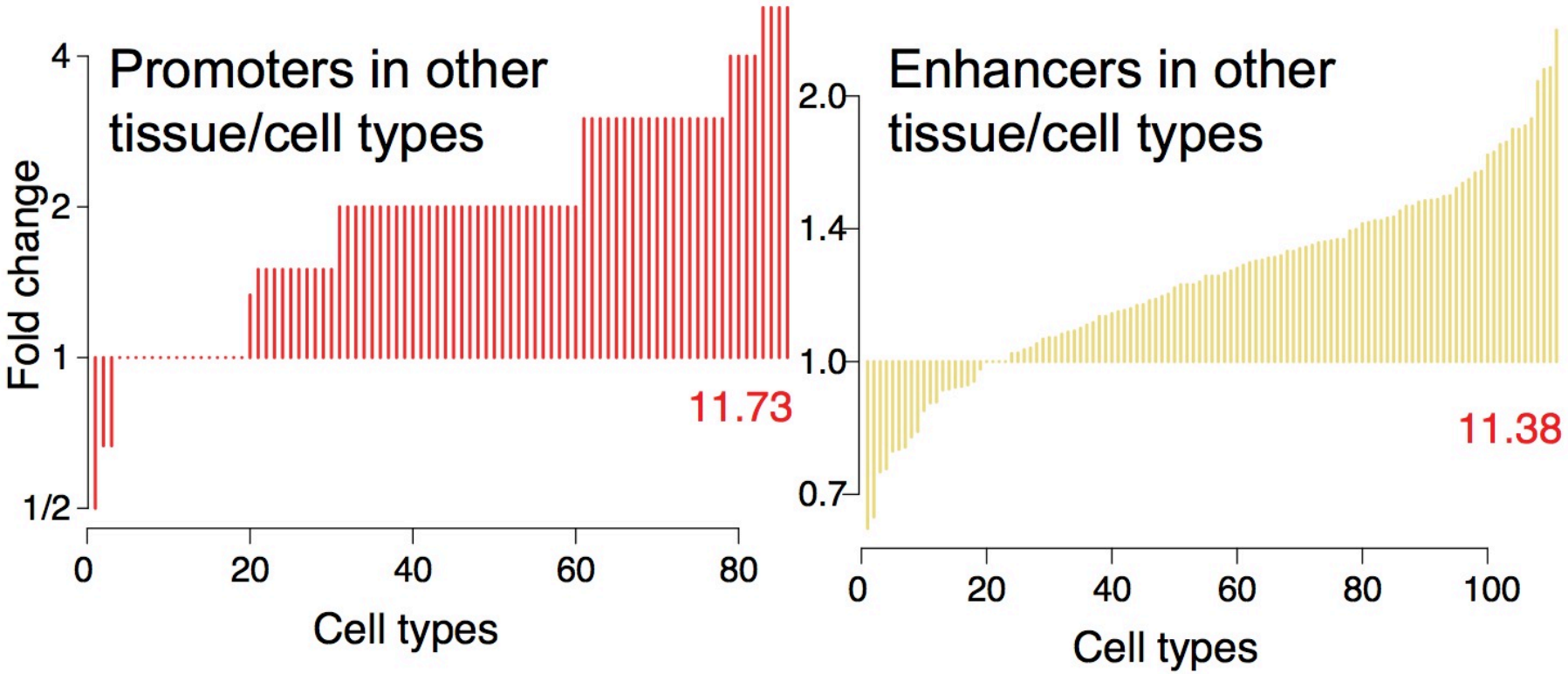

Disruptive mutations in ‘low’ elements are enriched in enhancers and promoters in other tissues

Out-of-context de-repression